INTERNATIONAL ATOMIC ENERGY AGENCY
UNITED NATIONS EDUCATIONAL, SCIENTIFIC AND CULTURAL ORGANIZATION

INTERNATIONAL CENTRE FOR THEORETICAL PHYSICS
34100 TRIESTE (ITALY) - P.O.B. 586 - MIRAMARE - STRADA COSTIERA 11 - TELEPHONE: 2240-1
CABLE: CENTRATOM - TELEX 460392 - I

SMR/390 - 21

WORKING PARTY ON "FRACTURE PHYSICS"
(29 May - 16 June 1989)

TRANSFORMATION TOUGHENING OF CERAMICS

Nils CLAUSSEN
Technische Universität Hamburg-Harburg
P.O. Box 901403
2100 Hamburg 90
Federal Republic of Germany

TRANSFORMATION TOUGHENING OF CERAMICS

Nils Claussen
Technische Universität Hamburg-Harburg
P.O. Box 901403
2100 Hamburg 90
Federal Republic of Germany

ABSTRACT. Ceramic materials can be considerably toughened by utilizing the phase transformation of ZrO_2 particles. The transformation is nucleation-controlled and invariably stress-assisted. Three main toughening mechanisms are operative: stress-induced transformation, microcracking and crack deflection. Some toughened ceramics with low critical transformational stress exhibit transformation plasticity and memory effects analogous to martensitic metal alloys. Microstructural features of the three ZrO_2 toughened ceramic (ZTC) groups are presented: Partially - stabilized ZrO_2 (PSZ), tetragonal ZrO_2 polycrystals (TZP) and dispersion -toughened ceramics, e.g. ZT-Al_2O_3, ZT-mullite, etc. The mechanical properties of some ZTC are compared with predicted values. Since ZTC generally exhibit a disappointing high-temperature behavior, some strategies are outlined to overcome the characteristic deficiencies.

I. INTRODUCTION

The mechanical properties of brittle ceramics can be improved by exploiting the tetragonal (t) → monoclinic (m) phase tranformation of discrete zirconia (ZrO_2) particles, precipitates or grains dispersed within ceramic matrices. The toughening originates essentially from the crack shielding associated with the volume and shape change of the martensitic transformation, which reduces the stress intensity at the crack tip. This type of energy dissipation is analogous to that associated with crack-tip plasticity in ductile metals.
The micromechanics of transformation toughening is understood in principle, but specific details in the several different types of transformation-toughened ceramic systems now known are still being debated. The least ambiguous toughening mechanism is that associated with the direct crack shielding provided by the stress-induced martensitic transformation in a zone ahead of propagating cracks (stress-induced transformation toughening). Another crack-shielding mechanism, which may lead to improved mechanical properties, is the nucleation and extension of matrix microcracks, themselves caused by

K. P. Herrmann and L. H. Larsson (eds.), Fracture of Non-Metallic Materials, 137–156.

the stress fields around transformed m-ZrO_2 particles. In this case, the transformation is induced thermally during cooling following fabrication (microcrack toughening).

A further toughening effect, which, other than crack-shielding, reduces the driving force for the crack propagation, involves crack deflection. The cracks can be deflected by localized residual stresses associated with transformed m-ZrO_2 particles or directly by t-ZrO_2 particles, e.g., at elevated temperatures (crack-deflection toughening). A further important aspect of stress-induced transformation is the generation of desirable residual compressive surface stresses from transformation induced e.g. by grinding or machining; this is analogous to surface strengthening of glass and can result in considerable strength increases (surface transformation strengthening).

The large-scale yielding of some highly toughened ZrO_2 ceramics has opened a completely new and technologically important field in ceramic materials. Large process zones and extended shear band formation make these ceramics flaw-insensitive, i.e., their strength is, as with metals, controlled by the yield stress. Furthermore, the similar shape-memory effect as exhibited in austenitic metal alloys can be utilized in technological operation.

Three basically different classes of ZrO_2-toughened ceramics (ZTP) have been identified: a) Partially-stabilized ZrO_2 (PSZ), in which t-ZrO_2 particles are coherently precipitated within a cubic (c) stabilized ZrO_2 matrix. b) Tetragonal ZrO_2 polycrystals (TZP) which consist predominantly of fine (< 1µm) t-ZrO_2 matrix grains. These ceramics have bend strength > 2000 MPa, and thus represent the strongest class of ceramic materials made to date; and c) Dispersion-toughened ceramics, where t- or m-ZrO_2 particles are dispersed in ceramic materials such as ZrO_2-toughened Al_2O_3 (ZTA), ZrO_2-toughened mullite (ZTM), ZrO_2-toughened spinel (ZTS), etc.

Throughout this article "ZrO_2-toughened ceramics" (ZTC) is used synonymously with "transformation-toughened ceramics", as virtually all work reported to date has focussed on ZrO_2 (or HfO_2-alloyed ZrO_2) as the "toughening" agent. It is possible that phase transformations in other materials may also be suitable for toughening ceramics.

A collection of literature on ZrO_2 systems and ZrO_2 toughening is contained in two conference proceedings /1,2/.

2. PHASE TRANSFORMATION

Pure ZrO_2 exists in three polymorphic forms. The high-temperature cubic phase with the fluorite structure is stable from the melting point, 2953 to - 2640 K. Between 2640 and 1440 K, a tetragonal distorted-fluorite structure is stable; below 1440 K, a further distortion to monoclinic symmetry occurs. It is generally accepted that the t → m transformation is martensitic in nature; the shape and volume increase (4.7% at room temperature) associated with this transformation invariably causes cracking in bulk ZrO_2. The start or M_s temperature of the bulk martensitic t → m transformation is ≤ 1220 K.

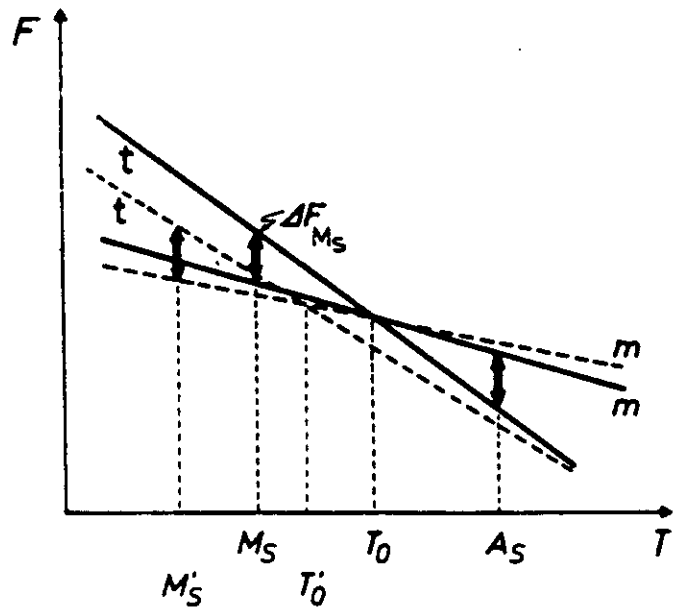

Fig. 1. Free energy (F) vs temperature (T) diagrams for martensitic reactions. t = parent phase, m = martensite phase. The solid and dashed curves are for pure ZrO_2 and ZrO_2 containing a stabilizer, respectively. T_0 and T'_0 are the temperatures where parent and martensitic phases possess the same free energy. ΔF_{Ms} is required for surmounting the nucleation barrier. M_S and M'_S are the martensite start temperatures, and A_S the temperature for the reverse transformation /3/.

Fig. 1 further explains the energetics of the transformation. The negative effects of this uncontrolled t → m transformation in bulk materials can sometimes be avoided if the c → t transformation can be suppressed. This can be accomplished by "stabilizing" the c structure by alloying additions such as MgO, CaO, Y_2O_3 or rare-earth oxides.

Extensive reviews of the transformation behavior, especially the nucleation of martensite (m-ZrO_2) in confined partials are given in references /3-6/.

2.1 Transformation in Confined ZrO_2 Particles

The situation is different for fine t-ZrO_2 particles, whether present as discrete grains or precipitates or particles included in a ceramic matrix. Firstly, M_S is lowered, often to below room temperature, and in some cases, to below 0 K. Secondly, the martensitic transformation within confined particles is invariably stress-induced; for toughening ZrO_2-containing ceramics, the stress fields associated with propagating cracks or with surface grinding or machining are most important.

The transformation of a confined particle is governed by two factors /5/: a) the free energy barrier involved in nucleation (ΔF^*); and b) the change of the total free energy of the system (particle plus matrix):

$$\Delta F = - \Delta F_O + \Delta U_T - \Delta U_I \qquad (1)$$

where ΔF_O is the chemical free energy change between parent ($t\text{-}ZrO_2$) and product ($m\text{-}ZrO_2$), which constitutes the driving force for the transformation, ΔU_T includes both the strain energy change and the changes in interface energy and ΔU_I is the interaction energy with the local stress. By increasing the driving force, e.g., by lowering temperature, or by changing ΔU_I by an externally applied stress, the transformation can be induced. For the reaction to take place, thermodynamic equilibrium has to be attained (ΔF 0) and the nucleation barrier must be overcome.

2.2 Nucleation of Martensite

The nucleation of "martensite" ($m\text{-}ZrO_2$), and hence the M_s temperature, is controlled by the size and shape of the particle, the chemistry of the system, the structure of the interface between matrix and confined particle, and the thermal expansion mismatch and elastic anisotropy of the system. The nucleation is invariably stress-assisted and heterogeneous, the stresses arising from thermal expansion mismatch between particle and matrix and any superimposed external stresses. For all particles other than perfect ellipsoids, stress concentrations are associated with shape inhomogeneities, e.g. grain facets, and scale with a characteristic particle dimension; this causes a particle-size dependent M_s temperature, and, for a given stress level, a particle-size-dependent propensity for transformation.

Fig. 2 further elucidates the size dependency of the transformation /7/. The left-hand side shows the free energies of pure ZrO_2 (m and t, cf. Fig. 1) and those of a small (F_1) and a larger (F_2) constraint t particle as a function of temperature. On the right-hand side, the respective free energies at room temperature are plotted versus the reaction coordinate. F_2 is at a higher energy level because the stresses controlling the elastic energy scale with the particle dimensions /8/. This energy term (see Eq. (1)) is

$$\Delta U_I = \varepsilon^T_{ij} \sigma_{ij} \qquad (2)$$

where ε^T_{ij} is the unconstrained transformation strain and σ_{ij} are the stresses due to a thermal expansion mismatch between particle and matrix or between differently oriented grains (TZP). Since $\Delta F^* \propto 1/\Delta F^2$, both, an increase in the driving force (ΔF_O) and/or an increase in internal (or external) stresses will promote the propensity for the transformation.

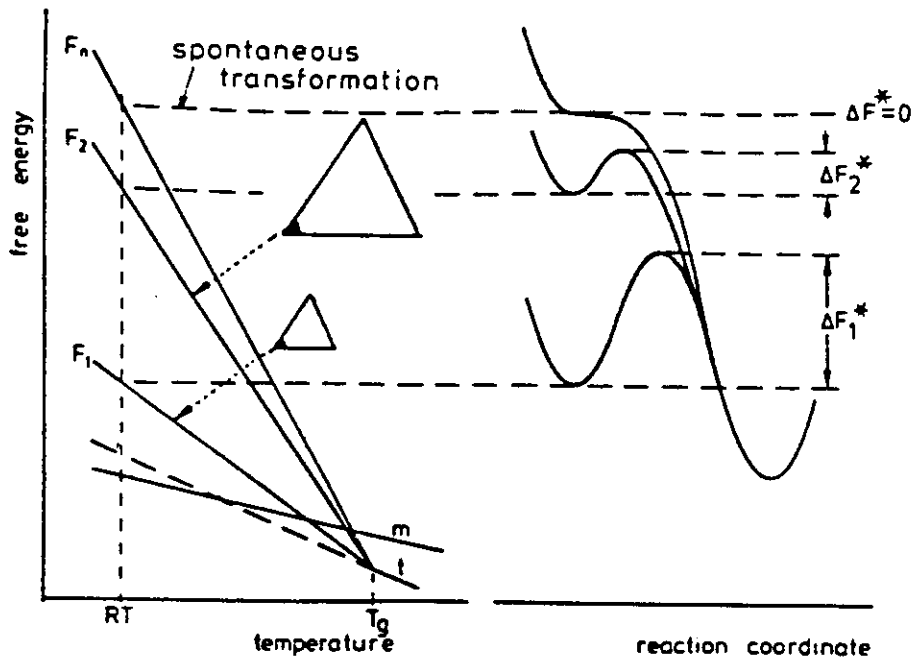

Fig. 2. Free energy vs temperature and vs reaction coordinate of a small (F_1) and a larger (F_2) constrained t-ZrO_2 particle. Since thermal expansion mismatch stresses scale with particle facett length F_2 is at a higher level than F_1. T_g is the temperature (~ 800°C) below which thermal stresses no longer relax.

3. TOUGHENING MECHANISMS

Toughening in ZrO_2-containing alloys may arise from several mechanisms associated with the transformation. The principal crack-shielding mechanisms are stress-induced transformation and stress-induced microcracking; these phenomena change the stress field around a crack tip such that the stress intensity factor is reduced. Thus, increased far field (external) stresses are necessary to propagate the crack, and the fracture toughness is increased. Crack deflection reduces the driving force for crack propagation, i.e., directly increase the critical crack-tip stress intensity factor.

Fig. 3 illustrates the crack shielding by a fully transformed or microcracked zone. The crack-tip stress ($K^{TIP}/\sqrt{2\pi r}$) is lowered by the transformation (or microcracking) provided the associated strain has the same sign as the crack-tip strain, i.e., the process zone volume must increase. The stress intensity in the near-tip region (K^{TIP}) is lower than the stress intensity due to the applied field, K^{∞}. The reduced stress intensity

$$\Delta K = K^{\infty} - K^{TIP} \qquad (3)$$

corresponds directly with an increased toughness. The crack propagates when K^{TIP} attains the toughness of the fully transformed or microcracked material, K_o. The toughness of the ZrO_2-toughened ceramic then becomes ($K^{\infty}=K_c$):

$$K_c = \Delta K_c + K_o \qquad (4)$$

In the following the toughness increment ΔK_c will be examined for stress-induced transformation and microcracking. K_o is changed both by crack deflection and microcrack degradation. Detailed analyses of the toughening mechanisms are presented by Evans et.al. /6,8-10/.

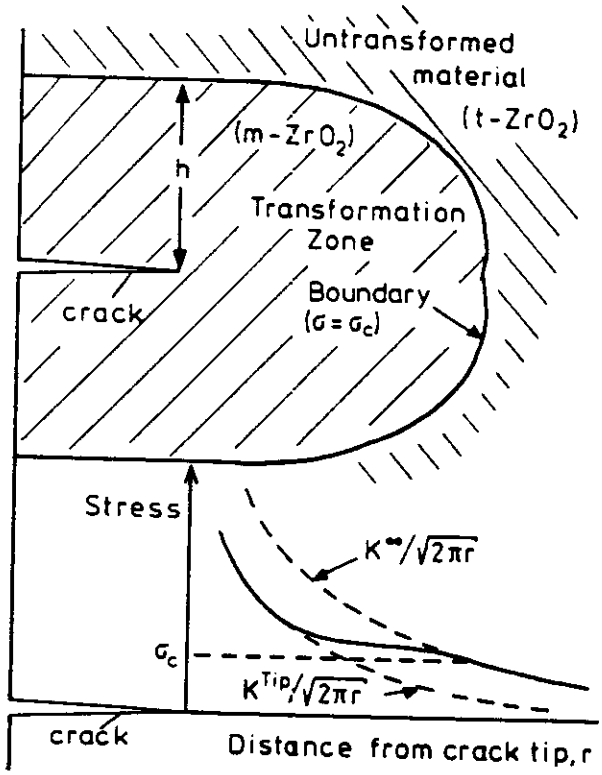

Fig. 3. a) Fully transformed or microcracked frontal process zone.
b) Modified stress field ahead of crack tip.

3.1 Stress-Induced Transformation

Stress-induced transformation is the dominant toughening mechanism in (PSZ) and (TZP) and less important in ZrO_2-containing dispersion-toughened ceramics. The prerequisite is the presence of t-ZrO_2 at the service temperature; as this is usually room temperature, M_s must be below room temperature. The toughening may be illustrated schematically as shown in Fig. 4.

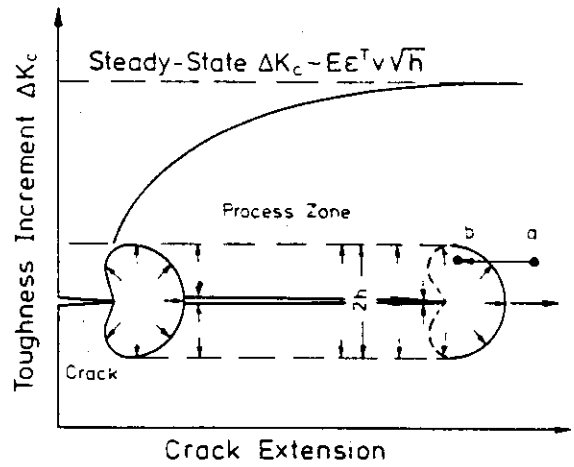

Fig. 4. Schematic diagram showing the development of the process zone with crack advance and the resultant toughness increment, ΔK_c; h is generally in the range 0.2-2 μm. Positions a and b of a volume element relate to the micrographs in Fig. 5.

On far-field loading of the crack, introduced in the untransformed material, the stress concentration around the crack tip will eventually reach a critical value at which the t-ZrO_2 particles within a "process" zone of width 2 h will transform. In the case of a dilational zone profile, ΔK determined by integrating the tractions along the transformation zone boundary, reveals that ΔK is zero, i.e., there is no toughening /10/ (This situation changes if a shear-band zone profile is considered).

On further loading, the crack has to propagate into the (compressive) process zone encountering enhanced crack resistance, i.e., ΔK increases, and consequently an R-curve is exhibited. After an extension of about 5 h, a steady-state toughness increment is attained, which, after integration of the traction over the transformation zone, is

$$\Delta K_c = c_{ij}\, v\, \varepsilon^T \sqrt{h} \qquad (5)$$

where c_{ij} is the elastic constant tensor and v the volume fraction of transformable t-ZrO_2. For purely dilatational transformation $c_{ij} = 0.22E/(1-\nu)$; this magnitude is more or less the same for reversible and inreversible transformation. If the transformation occurs in shear bands, $c_{ij} = 0.16E/(1-\nu)$ at the start of the propagating crack and $0.38E/(1-\nu)$ at steady-state /10,11/.

A volume element passing into the process zone (from position a to b in Fig. 4) interacts with the crack as shown experimentally in Fig. 5 /12/.

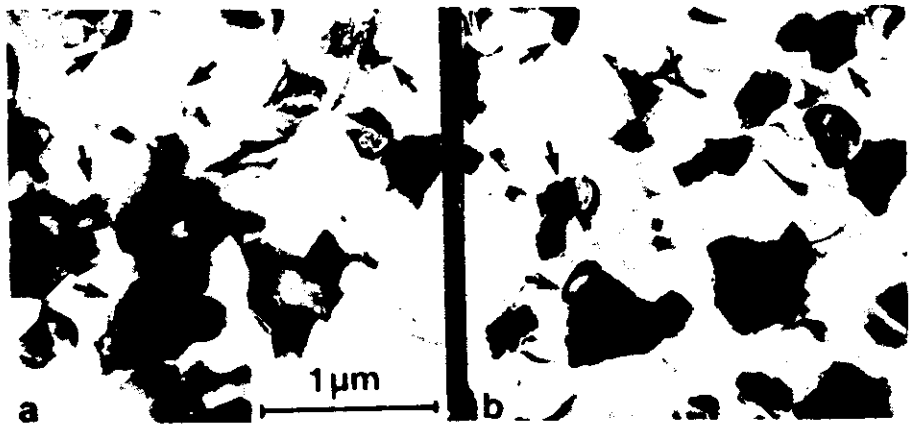

Fig. 5. High-voltage transmission electron micrographs of Al_2O_3 containing 15 vol. % ZrO_2 particles before (a) and after (b) loading by means of an in-situ straining stage. In the as-sintered composite, the ZrO_2 particles (arrowed) have t symmetry; after loading, most of them have transformed and undergone a characteristic twinning /12/.

This is a sample of a sintered ZrO_2-toughened Al_2O_3 containing 15 vol.% ZrO_2. Most ZrO_2 particles (arrowed) have t symmetry (Fig. 5a). After a critical stress is reached in the vicinity of the advancing crack, the particles transform (Fig. 5b). The transformed m-ZrO_2 particles are invariably twinned, the twinning occurring to minimize the shape strains accompanying transformation.

The process zone height is for the case of irreversible transformation:

$$h = \frac{\sqrt{3}}{12\pi} (1+\nu)^2 (K_c/\sigma_c)^2 \qquad (6)$$

where σ_c is the critical mean stress to initiate transformation.

The preceeding paragraph is based on a stress-intensity analysis, however, the same result can be derived applying thermodynamics of crack advance /6/. In the Griffith approach, the net energy increase associated with a crack increment occurs solely behind the crack tip and is expressed as a change in the interaction energy (cf. Eq. (2)). In front of the crack, a balance always exists between the decrease in interaction energy and the energy dissipated by the transforming particles.

The increment in the critical energy release rate is /6/

$$\Delta G_c = v \int_{-h}^{h} \Delta U_I^c \, dy \equiv 2 \, v\varepsilon T_{0c} h \tag{7}$$

which has been demonstrated to be identical to ΔK_c of Eq.(5) /11/. At transformation conditions it follows from Eq.(1):

$$\Delta U_I^c = - \Delta F_o + \Delta U_T \tag{8}$$

For a small transformation zone, $\Delta U_T \sim 0$, because the crack surface relaxes the transformation strain, then ΔU_I^c is directly related to the driving force which is experimentally observed when measuring ΔK_c or ΔG_c as a function of temperature (Fig. 6).

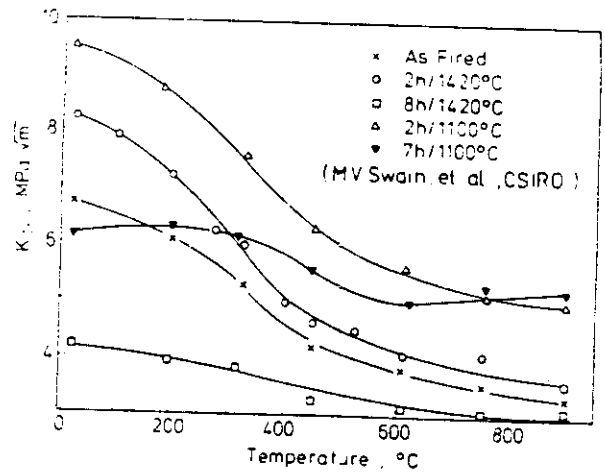

Fig. 6. Fracture toughness of various PSZ ceramics, heat-treated under different conditions, vs temperature /29/.

Another thermodynamic derivation of ΔG_c has been provided by Budiansky et.al./11/ by examining energy balance integrals. Again, no toughening is achieved as long as the crack does not extend into the transformed zone. However, when the zone is fully developed, the toughness increment derives as /6/

$$\Delta G_c = 2 \int_{o}^{h} U(y) \, dy \tag{9}$$

where U (y) is the residual energy density in the wake. U (y) can be evaluated using Fig. 7.

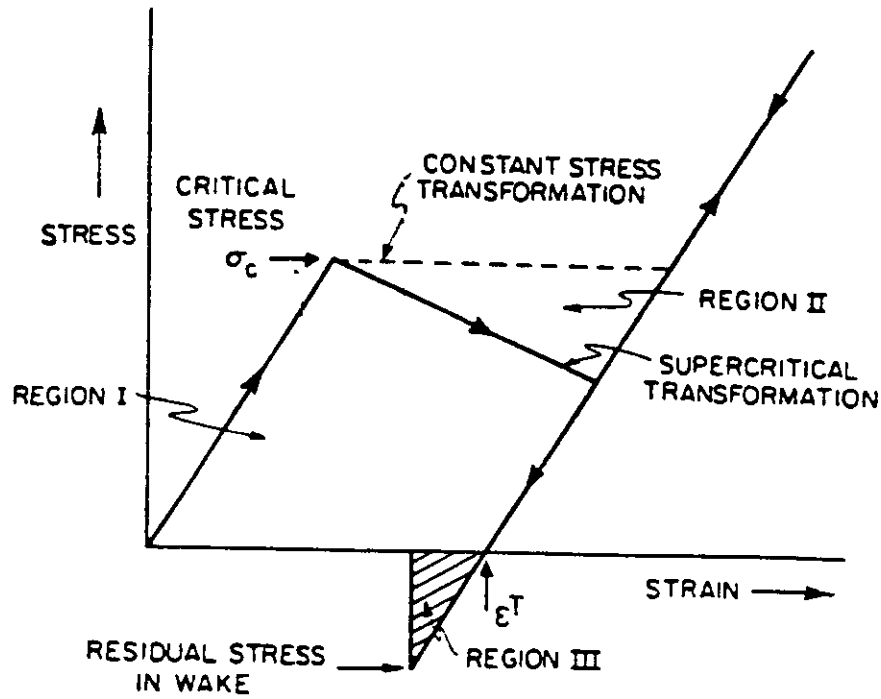

Fig. 7. Schematic stress-strain curve for supercritical martensitic transformation /6/. Hysteresis loop for a volume element (e.g. a in Fig. 4) passing through the process zone into the wake.

When passing from position a in Fig. 4 via b and beyond into the wake, a volume element undergoes a complete loading and unloading cycle. I.e., each volume element in the wake is subject to the residual stress work contained in the hysteresis loop in Fig. 7. The residual energy density is then represented by the areas of regions I, II and III. At supercritical transformation conditions (the stress drops below σ_c) the areas of II and III cancel. Then Eq. (9) is identical to Eq. (7).

3.2 Microcracking

Microcracking has been observed in all three ZTC types, i.e., PSZ, TZP and dispersion - toughened ceramics /13-17/, although it is more typical for the latter type where ZrO_2 particles are intergranularly dispersed.

Microcracks nucleate in regions of residual tension, hence, adjacent to transformed m-ZrO_2 particles, and due to thermal expansion mismatch. Relief of these stresses by extension, triggered by external loading, results in residual opening and associated dilatation. This dilatation is the main source of microcrack toughening /9,18/.

It can be shown that the volumetric strain induced by non-interacting microcracks is /18/:

$$\varepsilon^M = \frac{16\ (1-\nu^2)}{3}\ \frac{\sigma_R f}{E} \qquad (10)$$

where f is the microcrack density (correlates to the volume fraction of m-ZrO_2 particles if each particle is associated with one matrix microcrack), E is the modulus of the uncracked material and σ_R is the residual stress adjacent to ZrO_2 particles:

$$\sigma_R = (2/9)\ E\ \varepsilon^T\ /\ (1-\nu) \qquad (11)$$

The shielding and hence the toughness increment, ΔK_c can again be analyzed using the energy-balance integrals described in section 3.1 Fig. 8 shows the hysteresis loop for a volume element translating through the microcrack process zone (cf. Fig. 4). At the critical stress, σ_c, microcracks extend between ZrO_2 particles causing the dilatation, ε^M. On further loading and unloading the microcracked material exhibits a lower modulus than the uncracked material. The area under the loop corresponds to the energy density (cf. Eq. (9)).

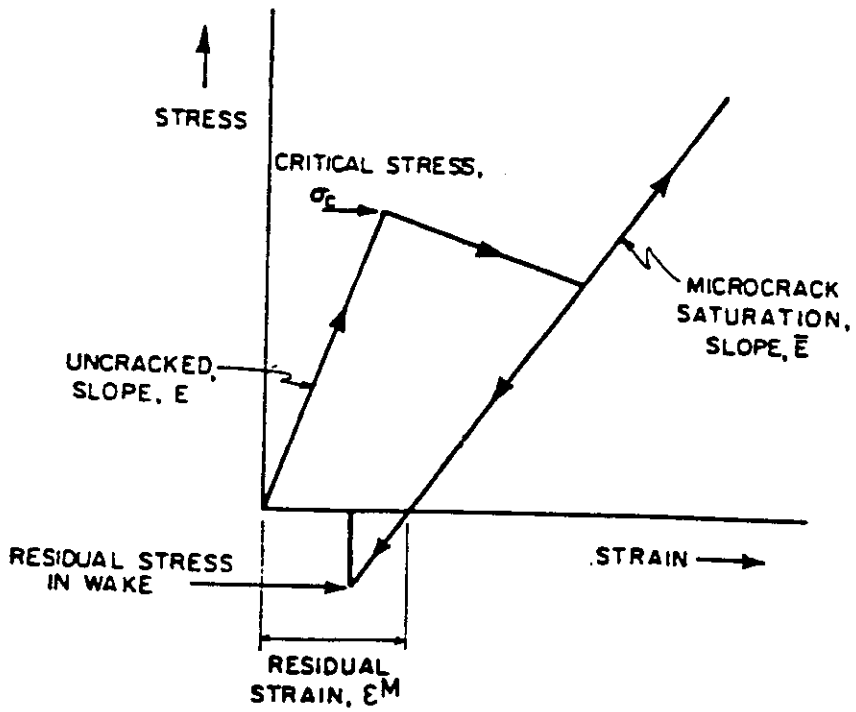

Fig. 8. Same schematic as in Fig. 7 for supercritical stress-induced microcracking. Note that the modulus of the microcracked material is reduced /6/.

In the case of pretransformed but uncracked material /6/,

$$\Delta K_c = \frac{0.07}{(1-\nu)} E \varepsilon^T \sqrt{h} (1.2 f^{1/3} - f) \qquad (12)$$

and for (less probable) simultaneous transformation and microcracking (Fig. 8)

$$\Delta K_c = \frac{0.14}{(1-0)} E \varepsilon^T \sqrt{h} (f + 0.6 f^{1/3}) \qquad (13)$$

Comparison with stress-induced transformation (Eq. (5)) shows that for equivalent h simultaneous transformation and microcracking is more effective than transformation alone. However, it must be noted that K_o in Eq. (4) is reduced by the microcracking by a factor (1-f) /6/.

3.3 Crack Deflection

Cracks can be deflected either by the residual stress fields associated with transformed m-ZrO_2 particle or by the fracture resistant t or m particles. The toughening results from the reduced driving force on the deflected portion of the crack /18,20/. The driving force can be estimated by separatly evaluating the mode I, II and III strain energy release rates /20/. The toughening magnitude depends on volume fraction and shape of the particles as well as the intensity of the associated stress fields. High-aspect ratio rods induce maximum toughness. Maximum toughening by a factor of 1.7 have been observed in ZrO-m-ZrO_2 alloys /21/.

The advantage of this mechanism is that it is independent of temperature and dictates K_o (Eq. 4)), hence, it adds to the ΔK_c of other mechanism. E.g., in whisker-reinforced ZrO_2 - toughened ceramics, K_o is considerably enhanced by cracks deflecting at the whiskers, while ΔK_c originates from stress-induced transformation /22/.

3.4 Surface Strengthening

The strength of ceramic materials can be increased by introducing compressive surface stresses, as is state of the art in glass technology. In ceramics containing ZrO_2, these stresses are produced by transforming particles in the surface layer to m symmetry and maintaining those in the bulk with t symmetry. This localized volume expansion can be stress-induced, i.e. by grinding, by sand blasting, or by a low-temperature treatment /23/.

Another method of producing these surface stresses is by chemically destabilizing t or c particles near the surface and allowing them to transform. Transient compressive stresses are generated on cooling composites containing m-ZrO_2 to room temperature. When composites are thermally shocked from temperatures LT > A_f, these transient compressive stresses counteract the thermal stresses and hence may completely prevent failure. E.g., Si_3N_4-ZrO_2 composites have been quenched from 1000°C into cold water without any measurable degradation. Some techniques for the introduction of compressive stresses are listed in Table 1.

Table 1. Possible technique for introduction of residual compressive stresses /23/.

Technique	Transformation induced	Example
Grinding, sand blasting, quenching	By stresses	Al_2O_3-ZrO_2, PSZ
Heat treatment	chemically	
in HfO_2 powder		Al_2O_3-ZrO_2
in air		Si_3N_4-ZrO_2
in vacuum		Mg-PSZ, Mg-CSZ, TZP
Cooling in liquid He or N_2 for short periods	Low-temp. quenching ($T_c<M_s$)	Al_2O_3-ZrO_2
Coating with (a) higher vol fraction, or (b) larger particle size	M_s of coating > T M_s of bulk < T, T: applic. temp.	Al_2O_3-ZrO_2

Although grinding-induced transformation is comparable to the transformation in the crack-tip stress field, the exact mechanisms have not been fully investigated. There are a number of possible mechanisms which may be simultaneously active: (a) Transformation is triggered by the high shear strains caused by the grinding process; (b) a high density of parallel flaws, induced by the abrasive media, creates similar stress-field transformations to those prevailing at single sharp crack tips; (c) the dislocations produced in the process pile up at particles and consequently cause their transformation. From various experiments with ZTA and ZTM ceramics it becomes obvious that surface grinding results in a much larger transformed depth than that due to crack propagation /25/.

Obviously, techniques that avoid the damaging of the surface have a greater potential for enhancing the strength /24/. However, grinding-induced surface strengthening is technologically more important since grinding is usually a required machining operation.

The residual compressive stresses at depth x (x : distance from the surface) can be estimated for a flat plate by /26/:

$$\sigma^C (x) = \varepsilon^T v_o e^{-bx} \cdot E/(1-\nu) \qquad (14)$$

assuming that the transformational depth is small with respect to the thickness of the plate, that the Young's moduli of matrix and particles are similar, and that the volume fraction of transformable particles is modest. v_o is the volume fraction of transformed m-ZrO_2 at the surface (x=0) and e^{-bx} is the transformation profile and b a constant. Surface stresses as high as 1 GPa have been measured in Al_2O_3-ZrO_2 (Y_2O_3) alloys /24/.

The strengthening magnitude depends on the residual compressive stress component of the stress intensity factor, K^R, the depth of the critical surface flaw with respect to the stress profile and the toughness of the material, K_c. At critical condition, the toughness of the surface - strengthened material is given by /27/

$$K_c^{ST} = K_c + K_c^R \qquad (15)$$

A detailed analysis of the strengthening by compressive surface stresses is presented in reference /24/.

3.5 Combined Toughening Mechanisms

Various toughening mechanisms can operate simultaneously. In some cases, they are additive, in others, counteracting. Due to the complexity it is rather difficult to account for the exact contribution of each specific mechanism. Generally, all shielding mechanisms can be expressed as /6/

$$K_c = \Sigma \sqrt{h} + K_o \qquad (16)$$

where Σ depends of the hysteresis or total crack closure forces. K_o is influenced by deflection and microcrack degradation. An alternative expression indicates a multiplicativity of shielding and reduction of crack-tip driving force /6/.

$$K_c = \left[\frac{0.046\ (1+\nu)\ E\ v\ \varepsilon^T}{(1-\nu)\ (\sigma_c - \sigma_r)} + 1 \right] K_o \qquad (17)$$

where σ_r is the residual stress in the zone. E.g., crack deflection requires an increase in applied load in order to bring K^{TIP} to the critical level (cf. Eq. (3) and (4)). Consequently, h increases which leads to additional stress induced transformation or microcracking.

In dispersion-toughened ceramics for instance, it has been shown that both microcrack and transformation shielding is operating, the respective extend depending on chemistry and size of the ZrO_2 particles /17/. In ZTA, the increases in toughness due to microcracking

are comparable to those achieved by the stress-induced t→m transformation /16,17/. The microcracking clearly occurs to relieve stresses introduced by the prior spontaneous t→m transformation, and at a given distance from a crack, is more likely to occur adjacent to the larger particles. Contrary to some previous theories, microcracking does not seem to accompany the stress-induced t→m transformation, i.e., a given particle can either transform in the stress field of a propagating crack, or if already transformed, can cause microcracking. If transformation occurs in a given stress field, the stress reduction so engendered does not permit microcrack nucleation /16/.

4. TRANSFORMATION PLASTICITY AND SHAPE-MEMORY EFFECT

It has recently been demonstrated that maximum strength of highly toughened ZrO_2 ceramics does not correlate with maximum toughness /37,28/, i.e., the basic fracture mechanical relation between strength, σ, and toughness

$$\sigma = Y K_c / \sqrt{C_f} \qquad (18)$$

no longer obtains. Y is a constant and C_f the fracture controlling flaw size. E.g., in a series of heat-treated Mg-PSZ ceramics, the peak strength invariably occurred at values between 50 and 75 % of the maximum toughnes /29/. Another example of this phenomenon was demonstrated with Y-TZP where the strength was considerably increased (to > 2000 MPa!) by the addition of Al_2O_3 while, at the same time, the toughness was reduced from 10 to 5 MPa $\sqrt{m}$ /30/.

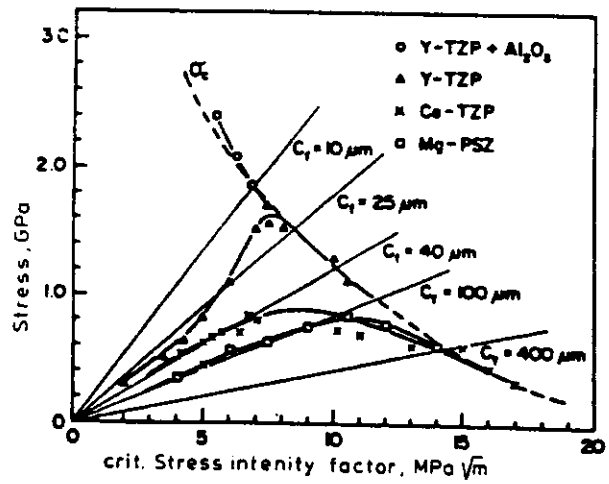

Fig. 9. Fracture toughness of several PSZ and TZP ceramics. The toughness of a specific alloy was changed by varying the heat-treatment. The plot indicates that the strength is limited by the critical stress to initiate the transformation, σ_c /28/.

Fig. 9 shows a collection of strength - toughness data for various PSZ and TZP ceramics /29/. It nicely demonstrates that the strength is limited by σ_c beyond a certain K_c value and becomes essentially insensitive to the preexisting flaw size. This is analogous to the mechanical behavior of steels in the ductile to brittle transition, where the inhomogeneity of the slip process causes microcracks to initiate at the yield strength. The microcracks rapidly become unstable and induce brittle failure /6/. In ZrO_2 alloys, the yield limited strength (yield limit equivalent to the critical stress to initiate transformation, σ_c) is probably controlled by the nucleation of microcracks which occur at shear band terminations /31/. The plastic strain at failure, manifested as a pronounced deviation from linearity in the stress/strain curves of Mg-PSZ /27/, may attain values of > 0.5 %, in certain TZP alloys even > 100 % when deformation is carried out at T > 1200°C /32/.

The prospect of yield-limited strength, as opposed to flaw-limited strength, implies an important change in the design philosophy of engineering parts, i.e., Weibull-statistics type of reliability considerations can be omitted /33/.

An interesting technological aspect of these "superplastic" ceramics is the utilization of large-scale plasticity as shape-memory parts /34/.

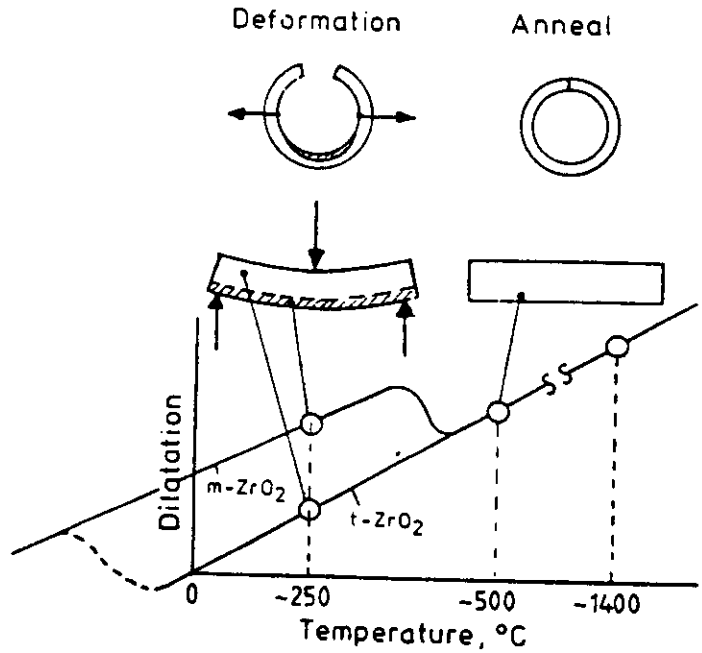

Fig. 10. Shape-memory effect in highly transformable Y-TZP ceramics. The stress and humidity induced transformation rate is a maximum at ca. 250°C.

In this case, Y-TZP is plastically deformed at low temperatures, i.e., the regions under high tensile and shear stresses are almost completely transformed to m symmetry (see example in Fig. 10).

The deformation process is usually carried out in the 250 to 300°C temperature range where the t → m transformation is especially enhanced in a humid atmosphere /14/. After heating the deformed part to $T > A_f$, the m part of the component is retransformed into the t form and consequently, the original shape is reasumed. This effect can be utilized in sensor devices, pipe fittings, high-temperature springs, etc.

5. TYPES OF TRANSFORMATION-TOUGHENED CERAMICS

Three basically different types of tough ZrO_2-containing ceramics have been developed: partially stabilized ZrO_2 (PSZ), tetragonal ZrO_2 polycrystals (TZP), and dispersion toughened ceramics /25/.

5.1 Partially Stabilized ZrO_2

PSZ ceramics contain insufficient solute (typically MgO, CaO or Y_2O_3) to prevent formation of t-ZrO_2; they are usually sintered in the c solid solution phase field, i.e., at relatively high temperatures ranging between ~1900 and 2100K, and consist of large (50-100 µm) c solid solution grains. During cooling, coherent t-ZrO_2 precipitates form and are usually coarsened or otherwise modified by aging at temperatures between 1370 and 1770K; this aging increases their propensity to transform under stress.

PSZ ceramics (mostly Mg-PSZ) have been items of commerce for some time, and have been optimized for high toughness and wear resistance. They find application as metal forming tools, dies, bearings, etc. and are being tested as automative components, such as came follower inserts, rocker faces, valve guides and seats, cylinder liners, piston caps, hot plates, etc. /35/.

5.2 Tetragonal ZrO_2 Polycrystals

TZP are fine-grained (0.1-1µm), predominantly single-phase fully dense t-ZrO_2 ceramics containing Y_2O_3 or rare-earth oxides. Sintering is optimally carried out in the t single-phase field; for example, 1.5 to 3.5 mole % Y_2O_3 alloys are sintered at temperatures between ~ 1600 and 1800K. This type of material is presently the toughest and strongest of all ZrO_2-containing ceramics, indeed probably of all polycrystalline ceramics made to date, with strengths > 2000 MPa and toughnesses > 10 MPa $\sqrt{m}$ having been achieved. The superior properties reflect the fine grain size and full density (probably achieved by the presence of a continuous glassy grain boundary phase), the lack of any intrinsic strength-limiting flaws and a very high volume fraction of the transformable phase. As for PSZ ceramics, they are

presently being tested as components in engines and as metal forming tools; furthermore, many new applications have been developed, such as scissors, knives, textile cutters, golf club inserts, etc..

5.3 Dispersion-Toughened Ceramics

The dispersion-toughened ceramics encompass a variety of two-phase materials containing mainly intergranular ZrO_2 particles. The critical ZrO_2 particle size for which M_s is < 300K varies with different matrices but is usually between 0.5 and 1.2 µm. Small amounts of Y_2O_3 are usually added to further stabilize the t phase.

The strongest representative of this class of material is ZrO_2-toughened alumina (ZTA), with strengths > 1000 MPa. Weaker matrices than Al_2O_3 - mullite, spinel, etc. - have been appreciably strengthened (> 500 MPa) by ZrO_2 additions. Commercial applications are cutting tool tips, high-performance seals, wear parts in heat engines, etc. /25/.

6. HIGH-TEMPERATURE PROBLEMS

Compared with the two currently available main competitors for high performance engineering ceramcis (SiC and Si_3N_4), ZrO_2-toughened ceramics have a clear advantage in the high applied stress regime, while the two covalent representatives exhibit a much greater high temperature potential. There are two principal reasons why the present ZrO_2-toughened ceramic (ZTC) types must be considered to be low temperature ceramics; firstly, the creep rates in the usually oxide-based ZrO_2-toughened ceramics (especially PSZ and TZP) are high relative to those of SiC and Si_3N_4 and, secondly, the most important toughening mechanism, which results from the stress-induced phase transformation, decreases drastically towards the equilibrium transformation temperature T_o (which is equal to about 1000°C for bulk ZrO_2, cf. Fig. 1).

This disappointing characteristic feature limits the load-bearing application of ZTC to low or, at the most, medium temperatures. Therefore, it represents a materials science challenge to search for wayse of improving the high temperature mechanical properties of these materials. The typical low temperature toughness of ZTC remains an important property even when they are used at higher temperatures, e.g. under thermal up shock and down shock conditions the maximum stresses usually occur at rather low temperatures. However, a better strength performance up to 1000-1200°C would considerably widen their technical use.

In a recent paper several strategies for strengthening ZTC for high-temperature application have been discussed /36/. The conclusion is that a number of possibilities exist to develop microstructures for ZTC in order to use this class of high performance ceramics at high temperatures. However, for further clarification of microstructural design criteria, it is important to investigate the high temperature thermomechanical behavior of the present ZTC types to a

greater extent, i.e. too little is known about the failure mechanisms, especially under static and dynamic stress conditions at elevated temperatures.

From the various strategies discussed the following measures seem to offer the best prospects for strength improvements at temperatures in the tetragonal stability range: (a) prevention or control of amorphous intergranular phases, i.e. by using high purity processing, by crystallizing the glass or by preventing the wetting of the grain boundaries; (b) addition of hard and high modulus second phases; (c) whisker (fiber) reinforcement, especially for TZP, ZrO_2-toughened mullite and ZrO_2-toughened cordierite.

REFERENCES

/ 1/ A.H. Heuer and L.W. Hobbs (eds.), Science and Technology of Zirconia, in Advances in Ceramis, Vol. 3, American Ceramic Society, Columbus, Oh, 1981.

/ 2/ N. Claussen, M. Rühle and A.H. Heuer (eds.), Science and Technology of Zirconia II, in Advances in Ceramics, Vol. 12, American Ceramic Society, Columbus, OH, 1984.

/ 3/ M. Rühle and A.H. Heuer, p. 14 ff in ref. 2

/ 4/ A.H. Heuer, N. Claussen, W.M. Kriven and M. Rühle, J. Am. Ceram. Soc., 65 (1982) 642.

/ 5/ A.H. Heuer and M. Rühle, to be published in Acta Met.

/ 6/ A.G. Evans and R.M. Cannon, to be published in Acta Met.

/ 7/ S. Schmander and H. Schubert, submitted to J. Am. Ceram. Soc.

/ 8/ A.G. Evans, Acta Met., 36 (1978) 1845.

/ 9/ A.G. Evans, p. 193 ff in ref. 2.

/10/ R.M. McMeeking and A.G. Evans, J. Am. Ceram. Soc., 65 (1982) 242.

/11/ B. Budiansky, J.W. Hutchinson and J. Lambropoulos, Int. J. Sol. Structures, 19 (1983) 337.

/12/ M. Rühle, A. Strecker, D. Waidelich and B. Krans, p. 256 ff in ref. 2.

/13/ A. King and P.J. Yarorsky, J. Am. Ceram. Soc., 51 (1968) 38.

/14/ M. Rühle, N. Claussen and A.H. Heuer, p. 352 ff in Ref. 2.

/15/ N. Claussen, J. Am. Ceram. Soc. 59 (1976) 49.

/16/ M. Rühle, N. Claussen and A.H. Heuer, to be published in J. Am. Ceram. Soc..

/17/ T. Kosmac, M.V. Swain and N. Claussen, Mat. Sci. Eng., 71 (1985) 57.

/18/ K.T. Faber, p. 293 ff in ref. 2.

/19/ J.W. Hutchinson, ref. 59 in ref. 6.

/20/ K.T. Faber and A.G. Evans, Acta Met., 31 (1983) 565.

/21/ H. Ruf and A.G. Evans, J. Am. Ceram. Soc., 66 (1983) 328.

/22/ N. Claussen, to be published in Fracture Mechanics of Ceramics, vol. 7/8, 1986.

/23/ N. Claussen and M. Rühle, p. 137 ff. in ref. 1

/24/ D.J. Green, F.F. Lange and M.R. James, p. 240 ff in ref. 2

/25/ N. Claussen, p. 325 ff in ref. 2

/26/ O. Richmond, W.C. Leslie and H.A. Wriendt, ASTM Trans. Q. 57 (1964) 294.
/27/ B.R. Lawn and D.B. Marshall, Phys. Chem. Classes, 18 (1977) 7.
/28/ M.V. Swain, J. Am. Ceram. Soc., 68 (1985) C 97.
/29/ M.V. Swain, to be published in J. Am. Ceram. Soc.
/30/ K. Tsukuma, K. Ueda and M. Shimada, J. Am. Ceram. Soc., 68 (1985) C 4.
/31/ Y. Fu, A.G. Evans and W.M. Kriven, J. Am. Ceram. Soc. 67 (1984) 626.
/32/ F. Wakai, GIRIN, personal communication.
/33/ I.W. Chen, to be published in J. Am. Ceram. Soc.
/34/ T. Soma and M. Matsui, Japanese Patent Appl. JP P131818-1983.
/35/ R.C. Garvie, p. 465 ff in ref. 2.
/36/ N. Claussen, Mat. Sci. Eng. 71 (1985) 23
/37/ M.V. Swain, to be published in Acta Met.